Single-Band 2-nm-Line-Width Plasmon Resonance in a Strongly Coupled Au Nanorod

ARTICLE *in* NANO LETTERS · OCTOBER 2015

Impact Factor: 13.59 · DOI: 10.1021/acs.nanolett.5b03330

NANO LETTERS

Letter

pubs.acs.org/NanoLett

Single-Band 2-nm-Line-Width Plasmon Resonance in a Strongly Coupled Au Nanorod

Pan Wang,[†,§] Yipei Wang,[†] Zongyin Yang,[†] Xin Guo,[†] Xing Lin,[†] Xiao-Chong Yu,[‡] Yun-Feng Xiao,[‡] Wei Fang,[†] Lei Zhang,[†] Guowei Lu,[‡] Qihuang Gong,[‡] and Limin Tong*[,†]

[†]State Key Laboratory of Modern Optical Instrumentation, College of Optical Science and Engineering, Zhejiang University, Hangzhou 310027, China

[‡]State Key Laboratory for Mesoscopic Physics, Department of Physics, Peking University, Beijing 100871, China

[§]Department of Physics, King's College London, Strand, London WC2R 2LS, United Kingdom

Supporting Information

ABSTRACT: This paper reports a dramatic reduction in plasmon resonance line width of a single Au nanorod by coupling it to a whispering gallery cavity of a silica microfiber. With fiber diameter below 6 μm, strong coupling between the nanorod and the cavity occurs, leading to evident mode splitting and spectral narrowing. Using a 1.46-μm-diameter microfiber, we obtained single-band 2-nm-line-width plasmon resonance in an Au nanorod around a 655-nm-wavelength, with a quality factor up to 330 and extinction ratio of 30 dB. Compared to an uncoupled Au nanorod, the strongly coupled nanorod offers a 30-fold enhancement in the peak intensity of plasmonic resonant scattering.

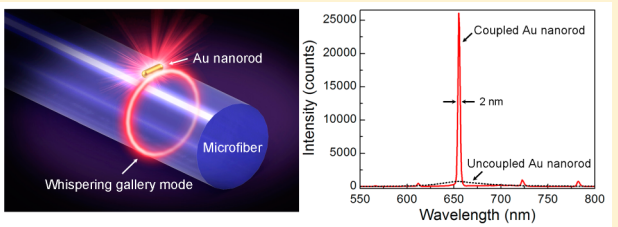

KEYWORDS: *Localized surface plasmon resonance, line width, whispering gallery modes, strong coupling, microfibers, Au nanorods*

Noble-metal nanoparticles are attractive materials due to their fascinating optical properties originated from localized surface plasmon resonance (LSPR) that is possible to confine light into the deep-subwavelength scale in all three dimensions. They have opened up a new realm of possibilities for a broad range of applications ranging from biological and chemical sensing,[1,2] nonlinear optical effects,[3] to nanolasers.[4,5] In general, it is desirable to have a higher resonance quality, plasmonic coherence, and field intensity in these nanoparticles for stronger light−matter interaction. However, in the resonance state, a plasmonic nanoparticle often suffers from both intrinsic metal absorption and radiative scattering losses,[6] which severely shorten the plasmon lifetime and subsequently broaden the resonance line width and deteriorate the coherence. As a direct measure of the quality of the plasmonic resonance, the line width of LSPR of metal nanoparticles is typically tens to hundreds of nanometers,[6,7] albeit narrower line width is highly desired for better performances in many applications.[1,4,8] For example, in most LSPR-based optical sensing, the detection limit and/or sensitivity is determined by the distinguishability of the spectral shift of the plasmonic resonance, which is in turn determined by the resonance line width. Therefore, narrowing the line width of the plasmonic resonance is one of the essential steps to push the limit of LSPR sensing. In the past years, great efforts have been devoted to modify the plasmon resonance of metal nanoparticles for spectral narrowing.[9−25] For example, using Fano interference in a nanoparticle cluster to get a narrow-line width dip,[9−11] patterning metal nanoparticles into arrays to realize diffraction coupling of localized plasmons,[12−16] or narrowing line width by coupling a metal nanoparticle with a photonic microcavity.[17−25] So far, the narrowest line width in nanoparticle plasmon resonance is observed in well-designed nanoparticle arrays and larger than 5 nm,[12−14] and the modified resonance spectrum usually contains multiple bands and obviously large background.

Here we demonstrate dramatically squeezing the LSPR band of an Au nanorod into an ultranarrow single resonance band by strongly coupling it with the whispering gallery cavity of an optical microfiber. As schematically illustrated in Figure 1a, the Au nanorod deposited on the surface of a microfiber acts as an optical antenna intercepting and concentrating incident electromagnetic energy into a small volume by plasmon resonance, and coupling it into the whispering gallery modes (WGMs) of the microfiber cavity (the efficiency of coupling free-space light directly into WGMs of the microfiber cavity is negligibly low due to the large momentum mismatch), forming a hybrid plasmonic−photonic coupling system. This is different from plasmonic nanoparticle−microcavity coupling systems where nanoparticles are directly excited by WGMs of the microcavities.[26,27]

Experimentally, Au nanorods were chemically synthesized using a seed-mediated method (see Supporting Information) and are relatively uniform in sizes with average lengths and

Received: August 19, 2015
Revised: October 11, 2015

DOI: 10.1021/acs.nanolett.5b03330
Nano Lett. XXXX, XXX, XXX−XXX

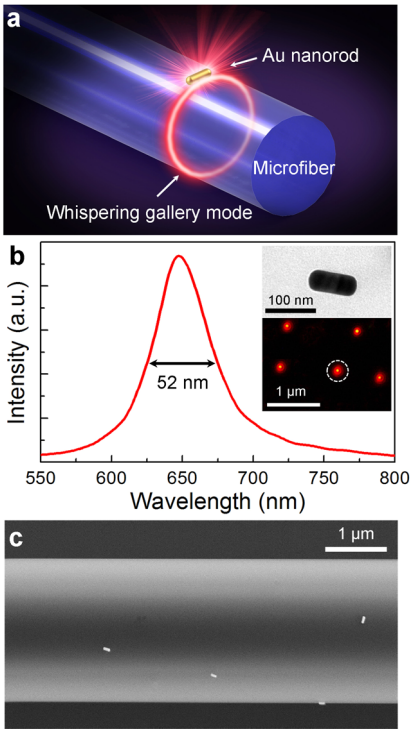

Figure 1. (a) Schematic diagram of coupling an Au nanorod with an optical microfiber. (b) Typical scattering spectrum of an Au nanorod deposited on a glass slide presenting a line width of ~52 nm. The insets show a TEM image of a typical Au nanorod (upper) and a dark-field scattering image of the measured Au nanorod (dotted white circled) (bottom). (c) SEM image of a representative experimental sample of a silica microfiber with several Au nanorods deposited on its surface.

diameters of 96 ± 8 and 37 ± 5 nm (upper inset of Figure 1b and Figure S1 in Supporting Information). The longitudinal surface plasmon resonance peak of an Au nanorod deposited on a glass slide (bottom inset of Figure 1b) is about 650 nm (Figure 1b), with a typical line width of about 52 nm.

Silica microfibers were fabricated by flame-heated taper drawing of standard optical fibers,[28] which can support high-quality-factor WGMs[29,30] owing to its atomic-level surface roughness[28] (see Figure S2 in Supporting Information). By immersing a microfiber into a dilute nanorod aqueous solution (1 pM) for a few seconds and drying it in the open air, we can deposit individual Au nanorods on the surface of the microfiber. Figure 1c shows a scanning electron microscopy (SEM) image of a 2.2-μm diameter microfiber; the four Au nanorods are well-separated from each other.

We used a side-illuminated dark-field spectroscopy[31] to investigate optical properties of single Au nanorods coupled to microfibers with diameters from 25.4 to 0.51 μm (see Figure 2a and Supporting Information). Figure 2b presents a typical optical microscopy image of an excited nanorod−microfiber system. The three-streak scattering traces around the 7-μm-diameter microfiber, corresponding well to the theoretical calculation,[30] clearly manifests the WGMs of the microfiber excited by the resonant nanorod (bright scattering dot).

When the microfiber diameter is relatively large (e.g., > 6 μm), the single-cycle dwelling time of photon in the microfiber cavity (>100 fs) is much larger than the lifetime of plasmons in the nanorod (~10 fs), and the coupled nanorod−microfiber system is in a weak coupling regime. Figures 2c−e show scattering spectra of single Au nanorods coupled to microfibers with decreasing diameters of 25.4, 11.2, and 6.38 μm, respectively. The drastic modulation of the scattering spectra is attributed to the coupling between LSPR modes of the nanorod and the WGMs of the microfiber, which agrees well with the resonance condition of a WGM microcavity (see

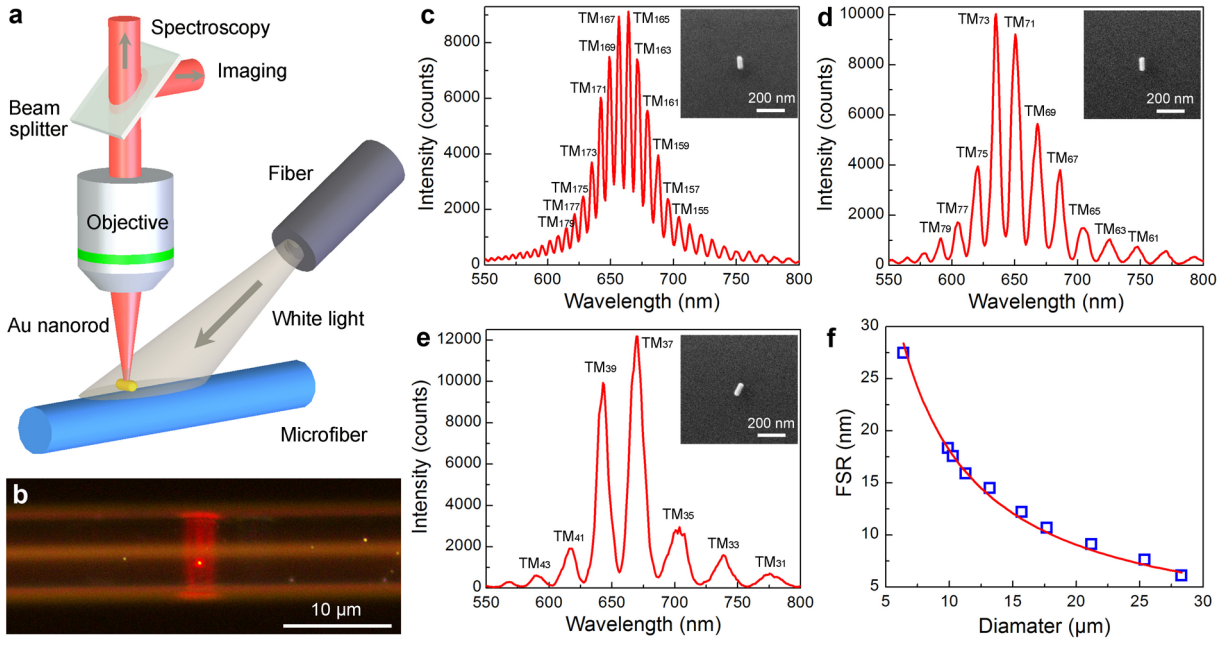

Figure 2. (a) Schematic illustration of the dark-field setup for light scattering imaging and spectroscopy of microfiber coupled single Au nanorods. (b) Optical microscopy image of an excited nanorod-microfiber coupled system. (c−e) Scattering spectra of single Au nanorods coupled to silica microfibers with diameters of (c) 25.4, (d) 11.2, and (e) 6.38 μm, respectively. Insets, SEM images of the corresponding Au nanorods on microfibers. (f) The dependence of FSR on the diameter of silica microfibers. The FSR curve fits well to a α/D function (α is ~187.8).

DOI: 10.1021/acs.nanolett.5b03330
Nano Lett. XXXX, XXX, XXX−XXX

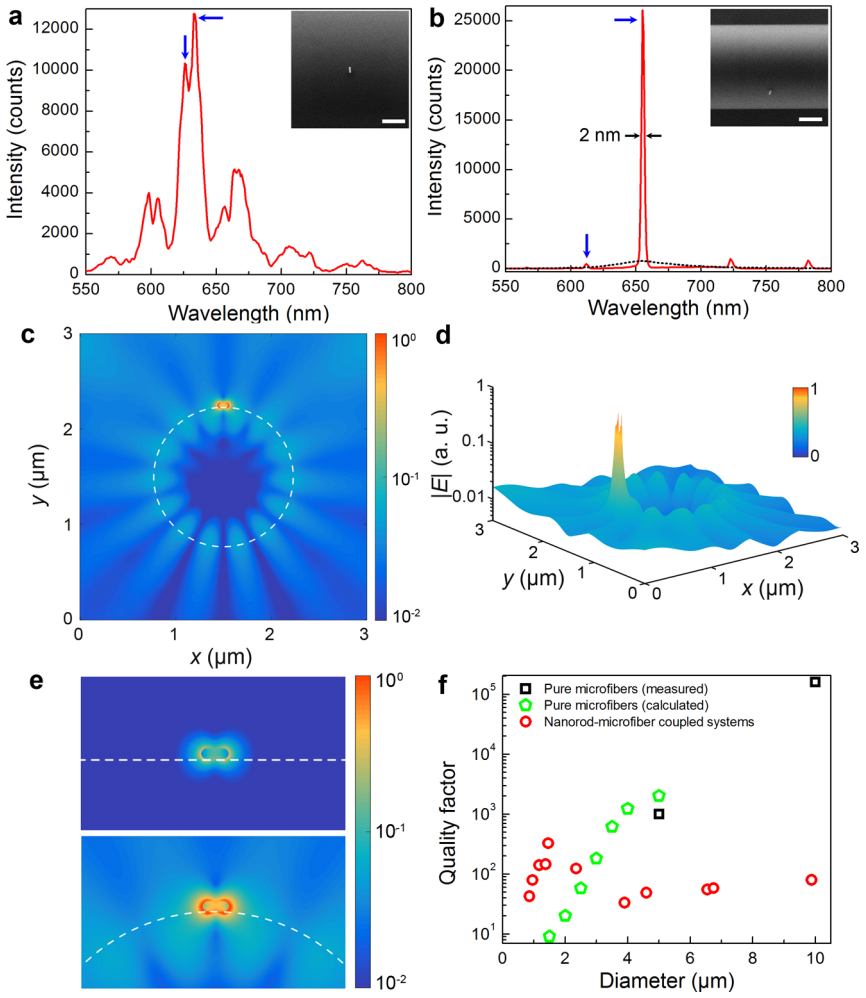

Figure 3. (a and b) Scattering spectra of single Au nanorods coupled to silica microfibers with diameters of (a) 5.6 and (b) 1.46 μm, respectively. Typical split doublets are indicated by blue arrows. Scattering spectrum of an Au nanorod on glass slide (black dotted line) is plotted as a reference in (b). Insets, SEM images of the corresponding coupled systems. Scale bars, 400 nm. (c) Simulated modal profile of the coupled nanorod-microfiber system in (b) at the resonance wavelength of 660 nm. The dimension of the Au nanorod is 100 × 40 nm. (d) Normalized electric field distribution of the coupled nanorod-microfiber system. (e) Comparison of the electric field distribution of uncoupled (upper) and coupled (bottom, same parameters as in c) single Au nanorod excited under the same condition. (f) Quality factors of pure microfibers (black hollow squares for measured results, green hollow pentagons for calculated results) and nanorod−microfiber coupled systems (red hollow circles) as a function of fiber diameter.

Supporting Information). The corresponding azimuthal mode numbers (m) of each resonance peaks are also presented in Figures 2c−e. The scattering peaks correspond well to the first order (radial number r = 1) transverse magnetic (TM) modes of the whispering gallery cavities. Also, due to the symmetry constraint of the coupled nanorod−microfiber system, only the odd TM modes are observed,[32] and the measured free spectral ranges (FSRs) of the scattering spectra are approximately twice that of WGMs of the microfiber.

The microfiber-diameter-dependent FSR (measured around 650 nm) of scattering spectra (Figure 2f) fits well to a α/D function, where α is a constant and D is the diameter of the microfiber. The measured α is ∼187.8, in good agreement with the calculated α of ∼185.6 (twice that of $\lambda^2/\pi n_{\text{eff}}$, where λ ∼ 650 nm and the effective index n_{eff} ∼ 1.45).

With smaller microfiber diameter, larger fractional energy of the WGMs circulates outside the microfiber as evanescent fields, which is beneficial for stronger coupling between the LSPR modes and the WGMs. Meanwhile, the plasmon lifetime becomes comparable to the single-cycle dwelling time of photons in the microfiber cavity (i.e., the energy stored in the plasmon cavity and the photonic cavity becomes comparable), leading to evident strong-coupling feature[33−35] with microfiber diameter below approximately 6 μm. Figure 3a shows scattering spectrum of a nanorod coupled to a 5.6-μm-diameter microfiber, in which mode splitting (one split doublet is indicated by blue arrows) of three resonance peaks is clearly seen. The mode splitting increases with decreasing microfiber diameter. When the microfiber diameter decreases to 1.46 μm, only one dominant line (m = 7) is left (Figure 3b, see more data in Figure S4 in Supporting Information), with mode splitting as large as 42.87 nm. All other lines (including the split doublets) shift to the edge or out of the plasmon resonance range. The measured line width of the single-band line is as narrow as 2 nm, giving a considerably large splitting-to-line width ratio of ∼21. For reference, scattering spectrum of a dielectric nanoparticle coupled to a microfiber contains much broader multibands (see Figure S5 in Supporting Information). Compared to that of an uncoupled Au nanorod (Figure 1b), the plasmon resonance of a strongly coupled nanorod shows a ∼ 25-fold reduction in line width. To the best of our knowledge, this is the narrowest line width of single noble-

DOI: 10.1021/acs.nanolett.5b03330
Nano Lett. XXXX, XXX, XXX−XXX

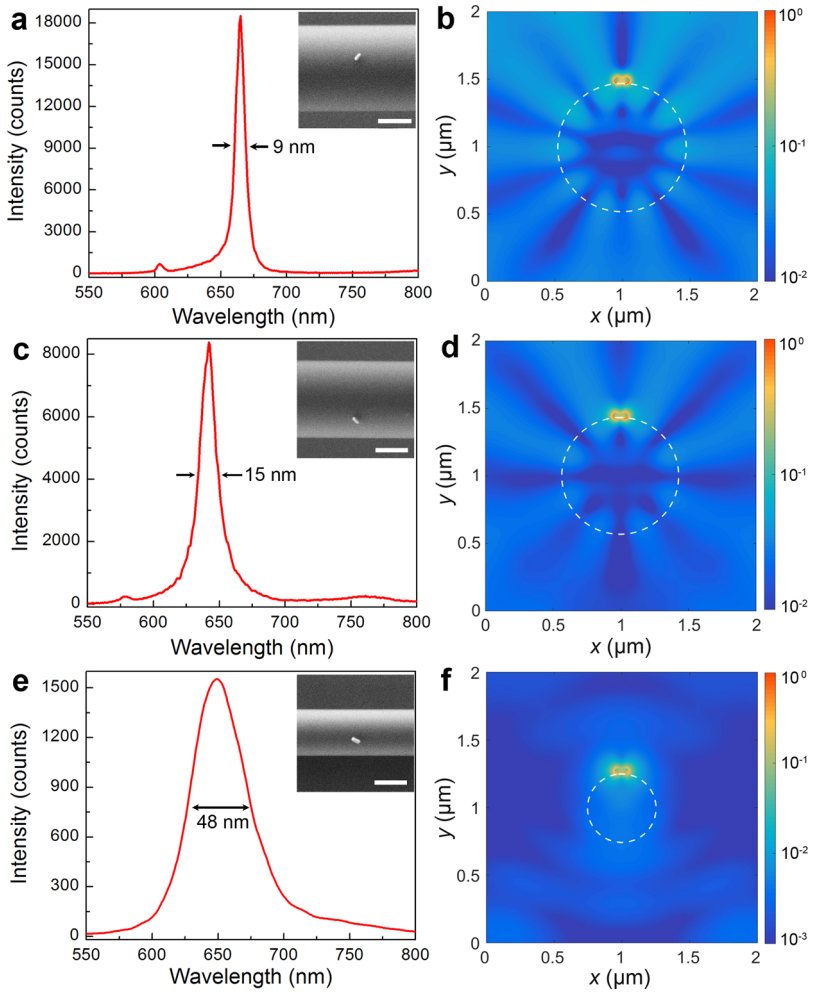

Figure 4. (a,c,e) Scattering spectra of coupled single Au nanorods and (b,d,f) corresponding modal profiles of the coupled systems with fiber diameters of (a,b) 950, (c,d) 860, and (e,f) 510 nm, respectively. Insets of (a,c,e), SEM images of the corresponding coupled systems. Scale bars, 400 nm.

metal nanoparticles that have ever been reported[6−8,19,23−25] and is also much narrower than those achieved based on nanoparticle arrays or clusters.[10−16] Moreover, unlike previous studies where the modified scattering spectra usually have an obviously large background,[11−16,23] the single-band scattering spectra shown here have almost zero background with a spectral contrast as high as 30 dB, indicating an almost complete energy exchange between the LSPR modes and the WGMs. Benefited from the broad tunable longitudinal surface plasmon resonance wavelength of Au nanorod,[36] the single-band ultranarrow resonance peak of the coupled Au nanorod can be readily tuned to a desired wavelength by changing the aspect ratio of the nanorod. It is worthy to mention that, despite the highly anisotropic optical property of individual Au nanorods, the single-band narrow resonance peak can be obtained at almost arbitrary nanorod orientations (Figure S6 in Supporting Information). Figure 3c and d present the simulated electric field distribution of an excited Au nanorod on the surface of a 1.46-μm-diameter microfiber (see details in Supporting Information), clearly showing the coupling between the LSPR modes and the WGMs: the LSPR radiation at both ends of the nanorod otherwise leaks into free space in an uncoupled Au nanorod (upper part of Figure 3e) and is efficiently coupled into WGMs and coherently recirculated back into the LSPR of the same nanorod (Figure 3c and bottom of part Figure 3e), which greatly elongates the plasmon lifetime, reduces the LSPR line width, and enhances the local fields in the nanorod. For comparison, under the same illumination condition, the measured peak intensity of the coupled nanorod (red solid line in Figure 3b) is about 30-fold stronger than that of a glass-slide supported Au nanorod (black dotted line in Figure 3b), which agrees very well with theoretical calculation (Figure 3e). The plasmon lifetime, estimated as $T = h(\pi\Gamma)$, where h is Planck's constant and Γ is line width,[6] is about ~230 fs.

Benefitted from the strong-coupling-induced reformation of the field distribution (Figure 3c) that localizes more energy inside the microfiber and reduces the radiation loss of both the plasmonic and photonic resonant modes,[37] the quality factor of the strongly coupled system is much higher than that of WGMs of a pure microfiber with same diameter (see Figure 3f and details in Supporting Information, for example, ~330 versus ~10 for microfiber with diameter of 1.46 μm), which is different with other nanoparticle−microcavity-coupled systems.[17−25] Therefore, the single-band ultranarrow-line width plasmon resonance is only possible in such a strong-coupled system: the significantly reduced loss leads to the narrow line width, and the large mode splitting together with the large FSR of the microfiber cavity keeps only one dominant line within

DOI: 10.1021/acs.nanolett.5b03330
Nano Lett. XXXX, XXX, XXX−XXX

the whole plasmon resonance range by pushing all other lines out of the resonance range.

It is also worthy to clarify that generally a 2-nm-line-width plasmonic scattering can be simply obtained by exciting an uncoupled nanorod using a 2-nm-line-width monochromatic light, but in that case there is no enhancement in plasmon lifetime,[38] quality factor, and field intensity compared with the strongly coupled nanorod we shown here.

When the microfiber diameter is reduced to below 1 μm, the leakage of the WGMs increases abruptly with decreasing diameter, resulting in obvious line width broadening of the plasmon resonance. As shown in Figure 4, with microfiber diameters decreasing from 950 nm (Figure 4a and b) to 860 nm (Figure 4c and d), the measured line width of the dominant plasmonic resonance increases from ~9 to ~15 nm (Figure 4b and d). The emergence of even mode (m = 4) in the 860-nm-diameter microfiber is due to the significant symmetry breakage of the field distribution in such a low-dimensional structure (Figure 4d). When the microfiber diameter is finally decreased to 510 nm (Figure 4e and f), the WGMs is no longer supported (Figure 4f), resulting in a 48-nm-width LSPR of the Au nanorod (Figure 4e), similar to that of the Au nanorod on a glass slide (Figure 1b).

So far we have realized single-band 2-nm-line-width plasmon resonance in a strongly coupled Au nanorod, which represents the largest elongation of plasmon lifetime in metal nanoparticles. The coupling scheme can be extended to plasmonic nanoparticles and microcavities of many other types, with the possibility of obtaining plasmon resonance with even narrower line width and greater versatilities. Meanwhile, the significantly reduced LSPR line width may open new opportunities for pushing the limits of plasmon-based techniques and inspiring better plasmonic devices such as ultrasensitivity nanosensors and ultralow-threshold plasmon lasers.

■ ASSOCIATED CONTENT

Supporting Information

The Supporting Information is available free of charge on the ACS Publications website at DOI: 10.1021/acs.nanolett.5b03330.

Synthesis of Au nanorods; side-illuminated dark-field spectroscopy; mode assignment; scattering spectra of microfiber coupled polystyrene nanoparticles; FDTD simulation; comparison of quality factors of pure microfibers and nanorod-microfiber coupled systems (PDF)

■ AUTHOR INFORMATION

Corresponding Author

*E-mail: phytong@zju.edu.cn.

Author Contributions

P.W. and Y.W. contributed equally to this work.

Notes

The authors declare no competing financial interest.

■ ACKNOWLEDGMENTS

The authors thank Xiaoshun Jiang for helpful discussions. This work was supported by the National Basic Research Program of China (No. 2013CB328703), the National Natural Science Foundation of China (Nos. 61475136 and 61036012), and the Fundamental Research Funds for the Central Universities.

■ REFERENCES

(1) Anker, J. N.; Hall, W. P.; Lyandres, O.; Shah, N. C.; Zhao, J.; Van Duyne, R. P. *Nat. Mater.* **2008**, *7*, 442−453.
(2) Mayer, K. M.; Hafner, J. H. *Chem. Rev.* **2011**, *111*, 3828−3857.
(3) Mühlschlegel, P.; Eisler, H. − J.; Martin, O. J. F.; Hecht, B.; Pohl, D. W. *Science* **2005**, *308*, 1607−1609.
(4) Noginov, M. A.; Zhu, G.; Belgrave, A. M.; Bakker, R.; Shalaev, V. M.; Narimanov, E. E.; Stout, S.; Herz, E.; Suteewong, T.; Wiesner, U. *Nature* **2009**, *460*, 1110−1112.
(5) Zhou, W.; Dridi, M.; Suh, J. Y.; Kim, C. H.; Co, D. T.; Wasielewski, M. R.; Schatz, G. C.; Odom, T. W. *Nat. Nanotechnol.* **2013**, *8*, 506−511.
(6) Sönnichsen, C.; Franzl, T.; Wilk, T.; von Plessen, G.; Feldmann, J. *Phys. Rev. Lett.* **2002**, *88*, 077402.
(7) Hu, M.; Novo, C.; Funston, A.; Wang, H. N.; Staleva, H.; Zou, S. L.; Mulvaney, P.; Xia, Y. N.; Hartland, G. V. *J. Mater. Chem.* **2008**, *18*, 1949−1960.
(8) Sherry, L. J.; Chang, S. − H.; Schatz, G. C.; Van Duyne, R. P.; Wiley, B. J.; Xia, Y. N. *Nano Lett.* **2005**, *5*, 2034−2038.
(9) Zhang, S.; Genov, D. A.; Wang, Y.; Liu, M.; Zhang, X. *Phys. Rev. Lett.* **2008**, *101*, 047401.
(10) Lassiter, J. B.; Sobhani, H.; Fan, J. A.; Kundu, J.; Capasso, F.; Nordlander, P.; Halas, N. J. *Nano Lett.* **2010**, *10*, 3184−3189.
(11) Yanik, A. A.; Cetin, A. E.; Huang, M.; Artar, A.; Mousavi, S. H.; Khanikaev, A.; Connor, J. H.; Shvets, G.; Altug, H. *Proc. Natl. Acad. Sci. U. S. A.* **2011**, *108*, 11784−11789.
(12) Kravets, V. G.; Schedin, F.; Grigorenko, A. N. *Phys. Rev. Lett.* **2008**, *101*, 087403.
(13) Zhou, W.; Odom, T. W. *Nat. Nanotechnol.* **2011**, *6*, 423−427.
(14) Shen, Y.; Zhou, J. H.; Liu, T. R.; Tao, Y. T.; Jiang, R. B.; Liu, M. X.; Xiao, G. H.; Zhu, J. H.; Zhou, Z. − K.; Wang, X. H.; Jin, C. J.; Wang, J. F. *Nat. Commun.* **2013**, *4*, 2381.
(15) Li, Z. Y.; Butun, S.; Aydin, K. *ACS Nano* **2014**, *8*, 8242−8248.
(16) Vitrey, A.; Aigouy, L.; Prieto, P.; García-Martín, J. M.; González, M. U. *Nano Lett.* **2014**, *14*, 2079−2085.
(17) Linden, S.; Kuhl, J.; Giessen, H. *Phys. Rev. Lett.* **2001**, *86*, 4688−4691.
(18) Christ, A.; Tikhodeev, S. G.; Gippius, N. A.; Kuhl, J.; Giessen, H. *Phys. Rev. Lett.* **2003**, *91*, 183901.
(19) Ameling, R.; Langguth, L.; Hentschel, M.; Mesch, M.; Braun, P. V.; Giessen, H. *Appl. Phys. Lett.* **2010**, *97*, 253116.
(20) Kekatpure, R. D.; Barnard, E. S.; Cai, W. S.; Brongersma, M. L. *Phys. Rev. Lett.* **2010**, *104*, 243902.
(21) Chanda, D.; Shigeta, K.; Truong, T.; Lui, E.; Mihi, A.; Schulmerich, M.; Braun, P. V.; Bhargava, R.; Rogers, J. A. *Nat. Commun.* **2011**, *2*, 479.
(22) Ahn, W.; Boriskina, S. V.; Hong, Y.; Reinhard, B. M. *ACS Nano* **2012**, *6*, 951−960.
(23) Schmidt, M. A.; Lei, D. Y.; Wondraczek, L.; Nazabal, V.; Maier, S. A. *Nat. Commun.* **2012**, *3*, 1108.
(24) Bahramipanah, M.; Dutta-Gupta, S.; Abasahl, B.; Martin, O. J. F. *ACS Nano* **2015**, *9*, 7621−7633.
(25) Konrad, A.; Kern, A. M.; Brecht, M.; Meixner, A. J. *Nano Lett.* **2015**, *15*, 4423−4428.
(26) Xiao, Y. − F.; Liu, Y. − C.; Li, B. − B.; Chen, Y. − L.; Li, Y.; Gong, Q. H. *Phys. Rev. A: At., Mol., Opt. Phys.* **2012**, *85*, 031805.
(27) Baaske, M. D.; Foreman, M. R.; Vollmer, F. *Nat. Nanotechnol.* **2014**, *9*, 933−939.
(28) Tong, L. M.; Gattass, R. R.; Ashcom, J. B.; He, S. L.; Lou, J. Y.; Shen, M. Y.; Maxwell, I.; Mazur, E. *Nature* **2003**, *426*, 816−819.
(29) Pöllinger, M.; O'Shea, D.; Warken, F.; Rauschenbeutel, A. *Phys. Rev. Lett.* **2009**, *103*, 053901.
(30) Sumetsky, M. *Opt. Lett.* **2010**, *35*, 2385−2387.
(31) Wang, P.; Zhang, L.; Xia, Y. N.; Tong, L. M.; Xu, X.; Ying, Y. B. *Nano Lett.* **2012**, *12*, 3145−3150.
(32) Rottler, A.; Bröll, M.; Schwaiger, S.; Heitmann, D.; Mendach, S. *Opt. Lett.* **2011**, *36*, 1240−1242.
(33) Ameling, R.; Giessen, H. *Nano Lett.* **2010**, *10*, 4394−4398.

DOI: 10.1021/acs.nanolett.5b03330
Nano Lett. XXXX, XXX, XXX−XXX

(34) Ameling, R.; Dregely, D.; Giessen, H. *Opt. Lett.* **2011**, *36*, 2218−2220.
(35) Ameling, R.; Giessen, H. *Laser Photonics Rev.* **2013**, *7*, 141−169.
(36) Ni, W. H.; Kou, X. S.; Yang, Z.; Wang, J. F. *ACS Nano* **2008**, *2*, 677−686.
(37) Chen, Y. − L.; Zou, C. − L.; Hu, Y. − W.; Gong, Q. H. *Phys. Rev. A: At., Mol., Opt. Phys.* **2013**, *87*, 023824.
(38) Puech, K.; Henari, F. Z.; Blau, W. J.; Duff, D.; Schmid, G. *Chem. Phys. Lett.* **1995**, *247*, 13−17.

DOI: 10.1021/acs.nanolett.5b03330
Nano Lett. XXXX, XXX, XXX−XXX